

# Variation of the in-plane penetration depth $\lambda_{ab}$ as a function of doping in $\text{La}_{2-x}\text{Sr}_x\text{CuO}_{4\pm\delta}$ thin films on $\text{SrTiO}_3$ : Implications for the overdoped state

J.-P. Locquet\*

*IBM Research Division, Zurich Research Laboratory, 8803 Rüschlikon, Switzerland*

Y. Jaccard

*IBM Research Division, Zurich Research Laboratory, 8803 Rüschlikon, Switzerland  
and Institut de Physique, Université de Neuchâtel, 2000 Neuchâtel, Switzerland*

A. Cretton and E. J. Williams

*IBM Research Division, Zurich Research Laboratory, 8803 Rüschlikon, Switzerland  
and Département de Physique de la Matière Condensée, Université de Genève, 1211 Genève, Switzerland*

F. Arrouy

*IBM Research Division, Zurich Research Laboratory, 8803 Rüschlikon, Switzerland  
and Institut of Inorganic Chemistry, University of Zurich, 8057 Zurich, Switzerland*

E. Mächler and T. Schneider

*IBM Research Division, Zurich Research Laboratory, 8803 Rüschlikon, Switzerland*

Ø. Fischer

*Département de Physique de la Matière Condensée, Université de Genève, 1211 Genève, Switzerland*

P. Martinoli

*Institut de Physique, Université de Neuchâtel, 2000 Neuchâtel, Switzerland*

(Received 2 April 1996)

Normal-state properties, such as the resistivity  $\rho_{ab}$  and the Hall coefficient  $R_H$ , structural properties, such as the  $c$  axis and in-plane lattice parameters, and superconductive properties, such as the critical temperature  $T_c$ , the penetration depth  $\lambda_{ab}$ , and the thermal activation energy for flux flow  $\Delta U$ , are reported for  $c$ -axis  $\text{La}_{2-x}\text{Sr}_x\text{CuO}_{4\pm\delta}$  films. These parameters have been measured as a function of doping in the range from heavily underdoped to heavily overdoped. The structural data indicate a 0.3% compression of the  $c$ -axis parameter and a corresponding 0.3% expansion of the in-plane lattice parameters as compared to bulk values, which explains the overall reduced critical temperature of these thin films. As the dopant content is increased, maximum values for  $T_c$ ,  $\Delta U$ , and  $\lambda_{ab}^{-1}$  are observed close to optimum doping, while  $R_H$  and  $\rho_{ab}$  decrease monotonically. [S0163-1829(96)06733-1]

## I. INTRODUCTION

It is of fundamental importance to establish the doping ( $x$ ) dependence of the superconducting properties in cuprate superconductors. Of particular relevance are the phase-transition line  $T_c(x)$ , which distinguishes the normal from the superconducting state, and the penetration depth  $\lambda(x)$ . Indeed a maximum  $T_c$  is observed for “optimum” doping, with a decrease in both the underdoped and overdoped regimes. The penetration depth  $\lambda$  characterizes the appearance of the Meissner state, and its “true” doping dependence is currently a topic of considerable debate.<sup>1-4</sup> On the other hand, from a phase-transition point of view, an analysis of thermal fluctuations points to three-dimensional (3D)  $xy$  critical behavior, which leads to a relation between the specific-heat singularity,  $\lambda$  and  $T_c$ , and predicts an increase of  $\lambda$  in the overdoped regime, independent of any microscopic mechanism of superconductivity.<sup>5</sup> Recent work on overdoped Tl compounds<sup>1,2</sup> and overdoped  $\text{YBa}_2\text{Cu}_3\text{O}_7$

“123” compounds<sup>6</sup> appears to confirm these predictions.

In this paper we report careful measurements of various properties on  $c$ -axis  $\text{La}_{2-x}\text{Sr}_x\text{CuO}_4$  (“214”) thin films, covering the doping regime from heavily underdoped to heavily overdoped. Particular attention was given to the preparation of *high-quality, homogeneous films*. First, the normal-state properties, such as the Hall coefficient  $R_H$  and the in-plane resistivity  $\rho_{ab}$ , are obtained as a function of doping; they allow an estimate of the mean free path  $l$ . Second, the evolution of the structural properties is reported as a function of doping and thickness. Then the thermal activation energy for flux flow,  $\Delta U$  — related to  $\lambda$  — is derived from  $\rho_{ab}(T)$  measurements in a magnetic field close to  $T_c$ . Finally, the in-plane penetration depth  $\lambda_{ab}$  is obtained directly from the kinetic inductance  $L_K$  for the same samples. About 20 samples have been characterized, and this work represents the most complete study of the behavior of  $\lambda$  from the heavily underdoped to the heavily overdoped regime to date.

The original Sr-doped  $\text{La}_2\text{CuO}_4$  compound<sup>7</sup> is an attrac-

tive material for such a study, as it supports “bulk” and homogeneous superconductivity over a large range of doping as recently demonstrated.<sup>8,9</sup> The preparation of “bulk” homogeneous “214” samples is tedious (particularly in the overdoped regime), owing to the very slow Sr incorporation into the easily formed undoped 214 lattice during solid-state sintering at the standard temperatures (more than 100 h are necessary for sintering at 900 °C).<sup>9</sup> This effect and the resulting “chemical phase separation” could well explain Uemura’s early results<sup>3</sup> as well as the claims that superconductivity is restricted to a narrow composition range.<sup>10,11</sup> From a sample-preparation point of view, the thin-film growth process is ideal for avoiding the occurrence of chemical phase separation. The growth process is mostly 2D, as films with large and atomically flat surfaces ( $\mu\text{m}$  size) can easily be obtained.<sup>12</sup> This indicates that the surface diffusion coefficients are certainly large enough to ensure a homogeneous Sr distribution. The films used here were grown on  $\text{SrTiO}_3$  using sequential molecular-beam deposition; the deposition details and the overall structural properties of the films have been published elsewhere.<sup>12,13</sup> Briefly, x-ray diffraction, atomic force microscopy, and transmission electron microscopy (TEM) revealed single-phase and  $c$ -axis single-crystal films with a surface roughness of about one unit cell (over  $1 \mu\text{m}^2$ ) and a microstructure that is essentially free of the usual defects observed in high- $T_c$  cuprate films, such as secondary phase inclusions,  $a$ -axis inclusions, grain and/or twin boundaries. Strong chemical inhomogeneity, such as that induced by large-scale Sr clustering, can be observed using TEM.<sup>13</sup> However during the TEM investigations of the films, no evidence of such behavior was found in the entire doping range studied.

## II. NORMAL-STATE PROPERTIES

The normal-state properties  $\rho^{-1}$  and  $R_H^{-1}$  obtained at 100 K using standard four-point and Hall-effect measurements are summarized in Fig. 1 as a function of doping. For both quantities a *monotonic increase* is observed with increasing Sr content. They are in *excellent agreement* with literature data of other thin films on  $\text{SrTiO}_3$  having a comparable thickness, although single crystals and thicker films show reduced resistivities ( $\approx 20\text{--}30\%$ ).<sup>14–17</sup> Higher resistivity values are typically taken as evidence of poor sample quality. On the other hand, the resistance ratio ( $\rho_{300 \text{ K}}/\rho_{50 \text{ K}}$ ) is also a good indicator for the quality of the thin films, and values between 3.3 and 3.5 were obtained for the optimally doped films. These values are as good as or better than those cited for the best films or single crystals reported so far, indicating a similar sample quality.<sup>17</sup> This apparent contradiction originates from a residual in-plane tensile stress, which expands the in-plane lattice constants and increases the resistivity to  $\approx 20\text{--}30\%$ . A quantitative argumentation is given below. We used the published  $R_H^{-1}$  values as a calibration curve to correct the experimental uncertainty ( $\approx 10\%$ ) in the Sr content of our films.

Models must be used to relate  $\rho^{-1}$  and  $R_H^{-1}$  to the carrier density  $n$ , and only the simplest ones predict a direct proportionality,  $\rho^{-1} \propto n$  and  $R_H^{-1} \propto n$ . Although more elaborate models could modify these predictions, we expect that  $\rho^{-1}$  and  $R_H^{-1}$  increase with  $n$ . Therefore our data suggest that the

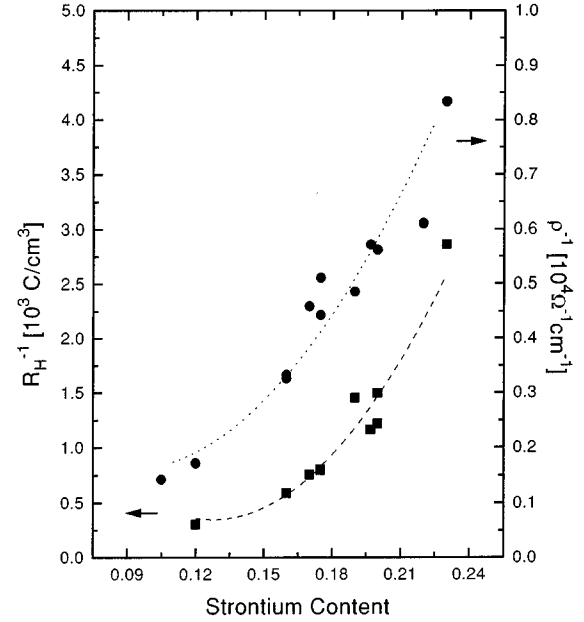


FIG. 1. Inverse resistivity (●) and inverse Hall coefficient (■) at 100 K versus Sr concentration.

carrier density increases with Sr doping. Further evidence of this comes from normal-state measurements of the Cu spin-lattice-relaxation rate, the magnetic shift and the spin susceptibility obtained from nuclear magnetic resonance (NMR) experiments on this compound<sup>18</sup> as well as on overdoped  $\text{YBa}_2\text{Cu}_3\text{O}_7$  (Ref. 19) and  $\text{Tl}_2\text{Ba}_2\text{CuO}_6$ .<sup>20,21</sup> These *independent* measurements clearly suggest that an increase in the Sr content indeed increases  $n$ .

## III. STRUCTURAL PROPERTIES

While the normal-state properties are in excellent agreement with literature values, there is a significant difference between the lattice parameters of 214 thin films on  $\text{SrTiO}_3$  and those of the bulk 214. From  $\theta$ - $2\theta$  x-ray-diffraction experiments, the value of the  $c$ -axis lattice parameter can be derived and is shown in Fig. 2 as a function of Sr content for our thin and thick films as well as for bulk samples.<sup>22</sup> These data are in very good agreement with those recently reported for laser-ablated 214 thin films on  $\text{SrTiO}_3$ .<sup>23</sup> Although there is an experimental error ( $\pm 0.01 \text{ \AA}$ ) in the determination of the  $c$ -axis lattice parameter for the thin films, a comparison between the data of films and bulk material indicates an average difference of  $\approx 0.045 \text{ \AA}$ , i.e., a contraction of about 0.35%. To compress the bulk 214 lattice to such an extent along the  $c$  axis, a pressure of 1.6–2.2 GPa (depending on Sr doping) would be necessary under *hydrostatic* conditions.<sup>24</sup>

There are two possible origins for this difference in lattice parameters. First, it is well documented that an oxygen deficiency in the 214 lattice gives rise to a reduced  $c$ -axis lattice parameter. This possibility can be excluded, as the samples are cooled under a flow of atomic oxygen that is sufficiently powerful to fill even some interstitial oxygen sites and that can induce superconductivity at 32 K in 214 thin films prepared without Sr,  $(\text{La}_2\text{CuO}_{4+\delta})$ .<sup>32</sup> In addition, a post-annealing of these films in an oxygen atmosphere at

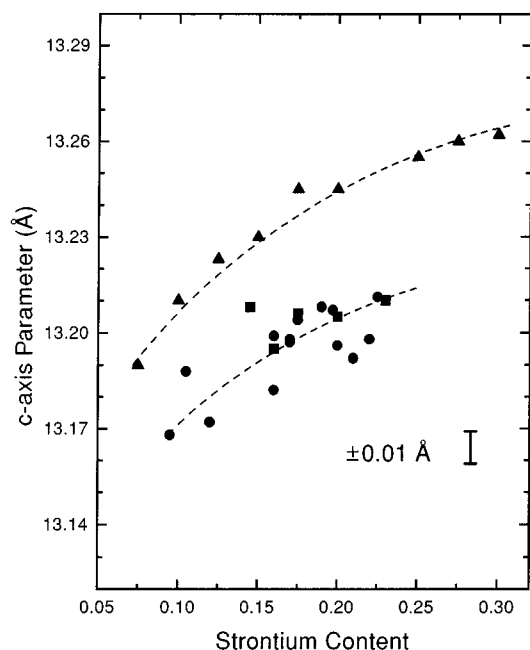


FIG. 2. Evolution of the  $c$ -axis lattice parameter versus Sr concentration for thick (■) and thin (●) films as well as for bulk samples (▲).

700 °C for 24 h does not significantly change the lattice parameters. The second possibility is related to the in-plane lattice parameter difference between  $\text{SrTiO}_3$  (3.9 Å) and 214 (3.8 Å). The 2.5% larger in-plane lattice parameter of the substrate could be partially responsible for the film in-plane lattice parameter extension, which would induce a shorter  $c$ -axis lattice parameter. During thin film growth such a large discrepancy between lattice parameters is usually accommodated by the appearance of misfit dislocations (for thicknesses larger than the critical thickness). For our 214 thin films, we have shown<sup>13</sup> that a regular network of misfit dislocations exists that accommodates “most” of the lattice misfit.

To find out whether the lattice misfit is completely accommodated by the creation of misfit dislocations, we have performed a detailed analysis of *in-situ* reflection high-energy electron diffraction (RHEED) spectra recorded during the deposition of an undoped 214 film on  $\text{SrTiO}_3$  at 750 °C. The RHEED images of the film present a series of long streaks at regular spacings, characteristic of two-dimensional growth.<sup>12</sup> Line scans taken across such spectra show a series of peaks that have been fitted using the Phearsen VII peak profile. From the peak positions the in-plane lattice parameter can be estimated *in principle* with an accuracy of  $\approx 0.01$  Å. However to obtain an accurate absolute value the precise geometrical diffraction conditions must be known. Minute geometrical changes of the sample manipulator during a temperature ramp currently prevent a measurement of the lattice parameters as a function of the temperature. Hence such a precision can only be maintained for a comparison under identical conditions (such as during growth). A more detailed report of this method and the analysis of the *in-situ* RHEED data is in preparation.<sup>25</sup>

To calibrate the vertical axis of Fig. 3 precisely we have used the lattice parameter of the substrate but extrapolated to

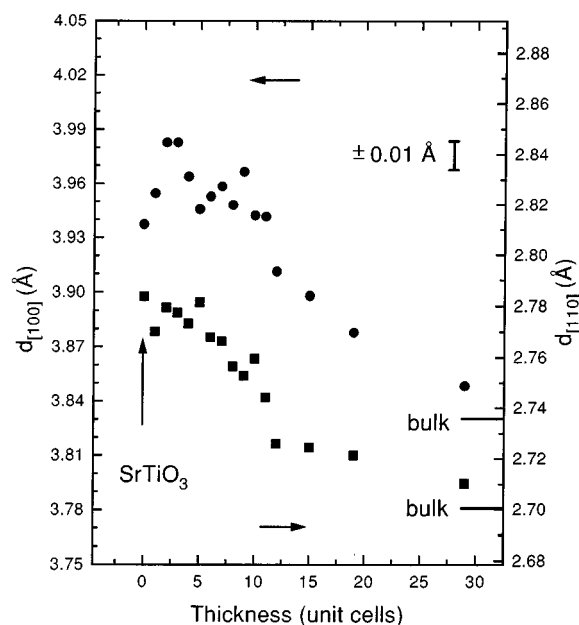


FIG. 3. Evolution of the in-plane  $d_{[100]}$  (●) and  $d_{[110]}$  (■) lattice parameters as a function of thickness for an undoped 214 film.

750 °C by using literature values of the thermal-expansion coefficients ( $\alpha$ ) of  $\text{SrTiO}_3$  and 214. For  $\text{SrTiO}_3$ ,  $\alpha \approx 11 \times 10^{-6}/\text{K}$ ,<sup>26</sup> which gives a  $d_{[100]}$  spacing of 3.937 Å. The only data we found regarding the thermal expansion of undoped 214 at temperatures much above the orthorhombic–tetragonal phase-transition temperature are given in Ref. 27, namely,  $\alpha \approx 8.5 \times 10^{-6}/\text{K}$  and a  $d_{[100]}$  spacing of 3.826 Å.

The evolution of the [100] and [110] lattice parameters is shown in Fig. 3 as a function of the number of unit cells deposited. The extrapolated bulk 214 values (3.826 and 2.703 Å, respectively) are indicated by the short lines on the right-hand axis. For the first unit cells (up to  $\approx 100$  Å), the in-plane lattice parameter is very close to that of the substrate. For larger thicknesses — as the creation of misfit dislocations sets in — a decrease of the lattice parameters is observed, but even at the maximum thickness studied here, there is no saturation. In addition, the thin-film values are still larger than the bulk lattice parameters, suggesting that the strain is not yet completely relieved. This remaining difference — averaged over the two data sets — corresponds to an in-plane lattice expansion of about 0.4%. Owing to the faster thermal contraction of the substrate as the sample cools after deposition, this mismatch might be reduced at room temperature. The misfit dislocations have been observed,<sup>13</sup> and their strain fields distort the film at the film/substrate interface over a typical distance of 2–6 unit cells, occasionally even up to 12 unit cells. Nevertheless careful measurement of the misfit-dislocation spacings<sup>28</sup> of Sr-doped 214 films has recently confirmed that strain remains present in the film.

Within the resolution ( $\approx 0.01$  Å) of the available instruments (x-ray diffraction, RHEED, and TEM), all thin films discussed here have a tetragonal structure. Even thin films of the undoped 214 compound — which has the largest orthorhombic distortion ( $b - a \approx 0.05$  Å) in bulk samples — show no deviation from the tetragonal symmetry. It is known that

the undoped orthorhombic 214 lattice can be transformed into a tetragonal lattice by the application of *hydrostatic* pressure of about 4 GPa.<sup>29</sup>

The above experimental data (the room-temperature *c*-axis lattice parameters, the high-temperature *in-plane* lattice parameters, and the absence of an orthorhombic distortion) unambiguously suggest that the thin films on SrTiO<sub>3</sub> are under tension. Unfortunately, these data were gathered under widely different experimental conditions, and with insufficient precision to allow a fully quantitative stress analysis. Qualitatively, however, the *cause* of this stress is an increased *in-plane* lattice parameter with a reduced *c*-axis lattice parameter as a *consequence*. Experimentally, an identical situation cannot be realized using high-pressure methods. In a uniaxial pressure experiment, cause and consequence are interchanged compared to our case, but similar changes in lattice parameters should be observed. Since no literature data are available regarding the evolution of the lattice parameters under uniaxial pressure, estimates from hydrostatic or quasihydrostatic experiments are used. The above lattice parameters show that the films are under tension, in a state that is qualitatively equivalent to the application of a *pseuduniaxial* pressure of the order of 2–3 GPa along the *c* axis.

As described by Goodenough and Manthiram<sup>30</sup> for the 214 compounds the La<sub>2</sub>O<sub>2</sub> sheets are under tension in the K<sub>2</sub>NiF<sub>4</sub> structure, because the eight La-O distances measured (three La-O distances  $\approx 2.52$  Å, five La-O distances  $\approx 2.714$  Å) are close to or larger than the sum of the ionic radii: 2.55 Å. However, the cohesion of the structure is ensured by the very short apical La-O bond ( $\approx 2.35$  Å). If the *a* and *b* lattice parameters increase — as is the case in our films — the lateral La-O distances should also increase, which therefore induces even more lateral tension in the La<sub>2</sub>O<sub>2</sub> sheets. In order to compensate such a stress, the apical La-O distances must decrease, corresponding to a decrease of the *c* axis in our thin films.

In the following paragraph we compare the normal-state properties of the films with those of bulk compounds under pressure. Unfortunately only few uniaxial-pressure measurements on the 214 compound exist. Therefore we make the reasonable assumption that the observed *in-plane* film properties are affected by the *in-plane* epitaxial tensile strain (i.e., a negative pressure) to a similar *magnitude* as is found under hydrostatic (positive) pressure for bulk compounds, but with *opposite sign*.

For the 214 system, it has been shown by Tanahashi *et al.*<sup>31</sup> that hydrostatic pressure has only a small effect (a few %/GPa) on the Hall coefficient over the entire doping range (0.08–0.24), which is in contrast to the sizable dependences found in the other hole-doped superconductors.<sup>24</sup> We are unaware of any uniaxial pressure Hall effect measurements, but a change of  $\approx 10\%$  in Hall coefficient is reasonable. For instance, those films that have a maximum critical temperature for a given thickness, show a Hall coefficient within 10% of the corresponding bulk value, suggesting that this effect is indeed small. Since we calibrated the actual Sr content in the films using the Hall coefficient of bulk samples, an uncertainty in the Sr content of our films is also expected. The changes in the resistivity under hydrostatic conditions are larger ( $\leq 10\%/GPa$ ) (Ref. 24) for this com-

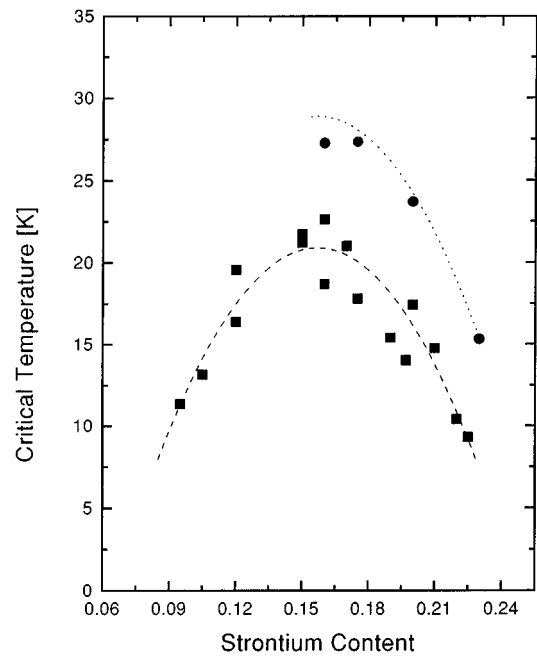


FIG. 4. The critical temperature as a function of Sr concentration for thin (■) and thick (●) films.

ound, and again, to our knowledge, no uniaxial measurements are available. However, since the *in-plane* lattice parameters increase, the *in-plane* resistivity ( $\rho_{ab}$ ) must increase accordingly, while the out-of plane resistivity ( $\rho_c$ ) and the anisotropy ( $\rho_c/\rho_{ab}$ ) must decrease. Further proof of this mechanism comes from the growth of 214 thin films on Sr-LaAlO<sub>4</sub> substrates, where the lattice mismatch is much smaller and in the opposite direction. In this case, the *in-plane* and *c*-axis lattice parameters are very close to the bulk values.<sup>25</sup> The resistivity of these thin films is indeed smaller ( $\approx 20$ –30%), in excellent agreement with those of thick films and single crystals and a high critical temperatures can be reached (38 K).

#### IV. CRITICAL TEMPERATURE

The critical temperature ( $T_c$ ) versus *x* was measured both resistively and inductively, and is shown in Fig. 4 for both thin (39, 50, and 65 nm) and thick (200 nm) films prepared under identical conditions. Typical transition widths — in both types of measurements — are 2–3 K, independent of the amount of doping. There is no evidence for a composition-dependent zero-field broadening of the transition. The maximum critical temperature observed, at optimum doping ( $x=0.16$ ) for the thickest films, is about 28 K; away from optimal doping, the critical temperature decreases. These data also confirm the well-known but not yet understood trend that the critical temperature of thin 214 films grown on SrTiO<sub>3</sub> strongly depends on the film thickness,<sup>14,17</sup> a  $T_c$  above 30 K being observed only for very large thicknesses.

Different structural phases with a different  $T_c$  occur in the 214 system as the structural details, such as the octahedral tilting angle and the orthorhombicity, are changed.<sup>33</sup> In thin films on a lattice-mismatched substrate, these parameters are

expected to differ from bulk values. The structural study presented here showed the presence of a significant tensile strain, which might explain — at least partially — the reduced critical temperature of these films. To our knowledge only one direct experiment of the uniaxial pressure dependence of the critical temperature is available in the literature: Motoi *et al.*<sup>34</sup> studied this property on grain-aligned 214 composites as a function of Sr doping and found that  $T_c$  decreases, at the rate of 3 to 9 K/GPa, under pressure applied along the  $c$  axis, depending on the doping level.

Alternatively the uniaxial pressure derivatives of  $T_c$  can be obtained by measuring the thermal-expansion anomalies at  $T_c$  along the different crystallographic orientations using the Ehrenfest relation. This method, which requires the knowledge of the specific-heat jump at the transition temperature, has been used by several authors,<sup>24,35–37</sup> and estimates of approximately  $-6$  to  $-7$  K/GPa for  $dT_c/dP_c$  (for pressure applied along the  $c$  axis), 2 K/GPa for  $dT_c/dP_a$ , and 5 K/GPa  $dT_c/dP_b$  have been reported for optimally doped samples. These data on bulk 214 samples, together with in-plane tensile strains equivalent to an estimated pseuduniaxial pressure of the order of 2 GPa, can easily explain the drastic reduction of the critical temperature in thin films to values around 20 K. A more quantitative analysis would require measurements of the pressure dependence of the critical temperature of both  $a$ - and  $c$ -axis 214 thin films as was done by Bud'ko *et al.*<sup>38</sup> for 123.

For thicker films more strain is relieved (although this is not clearly visible from the data in Fig. 2). The critical temperature is indeed higher, but the general trend of  $T_c$  versus  $x$  is the same for both thicknesses (see Fig. 4). Indeed, it is well known that applying pressure to this high- $T_c$  cuprate changes the *absolute values* of the critical temperature but does not affect the *general trend* of the superconducting properties (for instance, the maximum of  $T_c(x)$  still occurs for  $x \approx 0.16$ ). Applying a high-pressure oxygen treatment to such thin films can restore the bulk critical temperatures.<sup>39</sup> We did not perform such a treatment, as it introduces yet another process variable and as it can change the carrier density if additional oxygen is incorporated.

## V. COMPLEX IMPEDANCE MEASUREMENTS

To determine  $\lambda$ , several methods have been used, such as muon spin resonance ( $\mu$ SR) measurements,<sup>3</sup> ‘‘mixed-state’’ magnetization isotherms<sup>8,40</sup> [i.e.,  $M(H)$  in the reversible regime], and microwave experiments.<sup>41</sup> Here we derive  $\lambda_{ab}$  from a two-coil mutual inductance measurement.<sup>42</sup> This technique allows the complex sheet impedance  $Z_{\square} = R_{\square} + i\omega L_{\square}$  to be extracted from the measured real and imaginary parts of the signal using a numerical inversion procedure. In zero field,  $L_{\square}$  is the sheet kinetic inductance  $L_K$ , which is related to the penetration depth  $\lambda_{ab}$  by  $L_K = \mu_0 \lambda_{ab}^2 / d$ , with  $\mu_0$  the vacuum permittivity and  $d$  the film thickness. On the other hand,  $R_{\square} = \rho_{ab} / d$  is related to dissipation resulting from vortex motion.

### A. Activation energy

Close to  $T_c$  and in a magnetic field parallel to the  $c$  axis, we find that  $\ln \rho_{ab}$ , as inferred from resistive and inductive

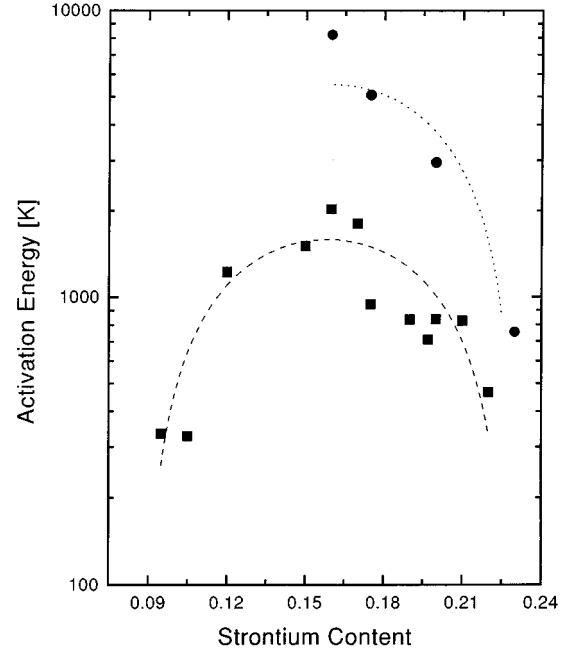


FIG. 5. The activation energy for flux flow  $\Delta U/k_B$  (expressed in temperature units) as a function of the Sr concentration for thin (■) and thick (●) films.

measurements, varies linearly with  $1/T$ , implying thermally activated vortex motion over a pinning barrier. The activation energies  $\Delta U(T=0)$  derived from the inductively measured  $\rho_{ab}(T)$  curves at  $H=0.4$  T are presented in Fig. 5 as a function of  $x$  for different film thicknesses. These data are very different from those reported in the literature,<sup>14</sup> where a large field broadening was observed in the underdoped regime, but not in the overdoped regime. We want to point out that the field used here (0.4 T) is much smaller and that the activation energy is obtained from  $\rho_{ab}$  values that are very close to the onset of resistance, in the resistivity range between  $10^{-3}$  and  $10^{-6} \mu\Omega$  cm, i.e., five to eight decades below  $\rho_{50\text{ K}}$  (see figures in Ref. 12). Hence these data cannot easily be related to those extracted from the broadening of the resistive transition in the  $100 \mu\Omega$  cm range and the doping dependence reported.<sup>14</sup>

In Fig. 5  $\Delta U$  reaches a maximum the height of which depends on the film thickness for optimum doping and decreases as one deviates from it. It is generally expected that  $\Delta U$  is proportional to  $1/\lambda^2$ . For instance, Feigel'man *et al.*<sup>43</sup> propose that the activation energy of a dislocation pair in the 2D collective-pinning model behaves as  $\Delta U = (\Phi_0^2 d / 16 \pi^2 \mu_0 \lambda_0^2) \ln(a_0 / \xi_0)$ ,<sup>44</sup> where  $a_0$  is the flux-line lattice spacing. Since  $a_0 / \xi_0 \gg 1$  at the field of interest in our studies, the logarithmic term is a slowly varying function of  $x$ , so that  $\Delta U(x)$  is essentially proportional to  $\lambda^{-2}(x)$ . Another relation was proposed by Blatter *et al.*<sup>45</sup> for the case of a single vortex along the  $c$  axis of a 3D superconductor containing randomly distributed, weak pinning centers:  $\Delta U = \Phi_0^2 \xi_0 \delta^{1/3} \varepsilon^{2/3} / 8 \pi^2 \mu_0 \lambda_0^2$ , where  $\delta$  is a disorder parameter and  $\varepsilon^2$  the mass anisotropy. Although  $\varepsilon$  is strongly doping dependent in the underdoped case, it becomes almost constant in the overdoped regime,<sup>8</sup> and therefore  $\Delta U(x) \propto \lambda^{-2}(x)$ . Thus the conclusion emerging from the data in

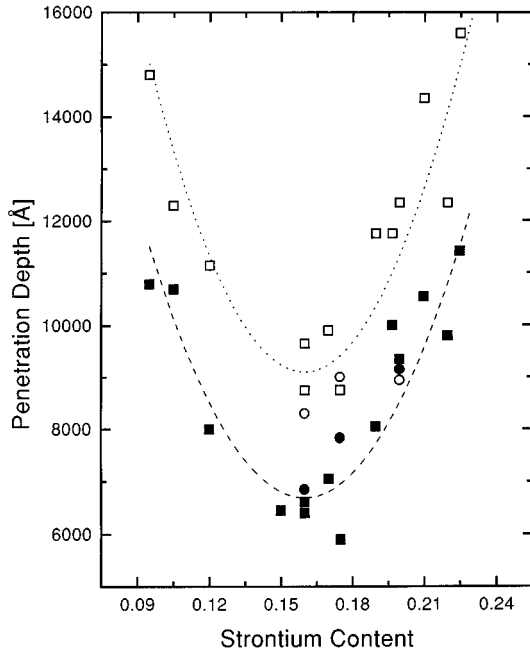


FIG. 6. The penetration depth  $\lambda_{ab}$  as a function of Sr concentration derived using the critical fluctuations close to  $T_c$  (■): thin and ●: thick films) and using a two-fluid extrapolation to 0 K (□: thin and ○: thick films).

Fig. 5 is that  $\lambda(x)$  is *nonmonotonic* in  $x$  with a minimum value at optimum doping. Stronger pinning, as suggested in Ref. 8, and/or a larger disorder  $\delta$  cannot explain the data in the overdoped regime.

### B. Penetration depth

Additional and even stronger evidence of the nonmonotonic  $\lambda^{-2}(x)$  with Sr doping is provided by direct measurements of  $\lambda_{ab}$  using the mutual-inductance technique. The temperature dependence of  $\lambda_{ab}(T)$  has already been published.<sup>12</sup> Except for the temperature regime close to  $T_c$  (where critical fluctuations play an important role), the temperature dependence can be fitted reasonably well with a two-fluid relation  $\lambda/\lambda_0(T)=[1-(t)^4]^{-1/2}$ , ( $t=T/T_c$ ), allowing the extrapolation of  $\lambda$  to  $T \rightarrow 0$  K. Figure 6 shows the extrapolated  $\lambda(0)$  (open symbols) as a function of doping. Fitting the same data with a BCS-type relation reduces the absolute values of  $\lambda(0)$  by  $\sqrt{2}$ , but does not change the doping dependence. Note that in the present context the detailed temperature dependence is unimportant, as the experimental data at a specific value of  $t$  are already sufficient to illustrate our point.<sup>12</sup> For instance, an alternative derivation of  $\lambda$  is provided by an analysis of the data close to  $T_c$ . In this region 3D fluctuations lead to a  $\lambda(T)/\lambda_0=[1-t]^{-1/3}$  dependence,<sup>5,12</sup> and values of  $\lambda_0$  have been included in Fig. 6 (filled symbols). It is expected that  $\lambda_0 \leq \lambda(0)$ , as observed experimentally, but regardless of the values used, a *nonmonotonic* behavior of  $\lambda(x)$  with a minimum close to optimum doping is obtained. The values for thick films confirm this observation and have also been included (●).

We do not place too much emphasis on the absolute values of the penetration depths obtained, as several experimen-

tal details render a comparison with bulk samples [where  $\lambda_{ab}(0) \approx 3000$  Å at optimum doping<sup>40</sup>] difficult. First, a simple relation between  $T_c$  and  $\lambda_0$  has been observed experimentally, namely the *Uemura plot*<sup>3</sup> that partially explains the large values of the penetration depth observed here: the values of  $\lambda_0 \approx 6000$  Å are simply due to the lower  $T_c$  between 20 and 30 K.<sup>3,4,8</sup> Indeed, this experimental correlation yields a relation between  $T_c$  and  $\lambda_0$  of optimally doped cuprate superconductors:  $T_c \propto \lambda_0^{-2}$ . Hence, rather than a bulk  $\lambda_0$  value of  $\approx 3000$  Å, our films would ideally have a  $\lambda_0$  value of  $\approx 4200$  Å, close to what we actually observe.

Secondly, to deduce  $\lambda_0$  from the measured  $L_K$ , we have used the nominal film thickness. Actually, on account of the presence of strain fields which suppress superconductivity in those portions of the film which are close to the substrate, the effective thickness where superconductivity is established homogeneously might be less than the nominal one, thereby leading to smaller values of  $\lambda_0$ .

Thirdly, the equation<sup>42</sup> used to derive the value of  $L_K$  from the inductive measurements is valid for shielding currents extending over very large radii. The lateral dimensions of our thin films (1 cm<sup>2</sup>, i.e., only 2–3 times larger than the driving-coil diameter) will certainly affect the shielding efficiency, which might lead to higher values of the penetration depth.

Finally, we have shown that the films are subject to an in-plane *epitaxial tensile strain* that reduces  $T_c$ . It is not known to what extent this strain influences the absolute values of the penetration depth or its anisotropy ( $\lambda_{ab}/\lambda_c$ ). In any case, the first argument is certainly valid, and the remaining difference between the bulk and our thin-film values (4200–6000 Å) is probably due a combination of the three other experimental constraints. As the remaining difference is rather small, *the observed behavior is intrinsic and cannot be an artefact due to the sample quality.*

These different experimental constraints are not expected to be a strong function of doping, thus we focus on *the general trend of the data* as a function of Sr content rather than on the absolute values. For instance, when comparing our film data in the underdoped regime to those available for bulk samples,<sup>3,4,8</sup> the same experimental trend can be observed [in both cases  $\lambda(0)(x=0.1)/\lambda(0)(x=0.16) \approx 2$ ]. In the overdoped regime, values of  $\lambda$  are difficult to obtain for bulk samples.<sup>8</sup> The thin-film data presented here are the first for heavily overdoped 214 samples, and *the excellent agreement between the films and bulk samples in the underdoped regime suggests that the observed nonmonotonic behavior in the overdoped regime is an intrinsic property of this compound.*

## VI. DISCUSSION

The results obtained from resistive and inductive measurements indicate that, despite the fact that more carriers are being added to the system, the screening capability of the superconductor is reduced in the overdoped regime. *This is the main result of our paper and is in marked contrast to the simple London prediction  $\lambda_{ab}^{-2} \propto n_s/m^*$ .* This effect has also been observed in overdoped Tl and 123 compounds.<sup>1,2,6</sup>

### A. Dirty limit

Such a behavior could be expected for a superconductor in the dirty limit ( $l \ll \xi_0$ ), and estimates indicate that  $l$  must be smaller than  $\xi_0/10$  in order to explain the observed upturn. The mean free path in the 214 system has been estimated from resistivity<sup>46</sup> and infrared<sup>47</sup> measurements. From the resistivity measurements a value of  $\rho \times l = 3 \times 10^{-10} \Omega \text{ cm}^2$  has been derived for an optimally doped sample. For the regime of interest (optimally to overdoped), our  $\rho$  values — close to  $T_c$  — are between 100 and 200  $\mu\Omega \text{ cm}$ , which gives a mean free path of 300 to 150  $\text{\AA}$ , respectively. The infrared measurement of a thick, optimally doped 214 film (8200  $\text{\AA}$ ) close to  $T_c$ , led to an estimate of  $l \approx 275 \text{\AA}$  a value that is in agreement with the resistivity measurement. From these estimates, it is clear that  $l$  is much too large compared to the quoted short coherence length in these cuprates, to explain the observed upturn in  $\lambda$ .

### B. 3D $xy$

The results are consistent with the analysis of thermal fluctuations close to  $T_c$  (3D  $xy$  critical behavior), which leads to a relation between the specific-heat singularity,  $\lambda$  and  $T_c$ .<sup>5</sup> With this relation,  $\lambda$  can be derived from the specific-heat singularity and  $T_c$ ,  $T_c \propto \lambda_0^{-2}$ , and an increase of  $\lambda$  in the overdoped regime is predicted, *independent of any microscopic mechanism of superconductivity*. Hence, the 3D  $xy$  behavior extends over the entire phase-transition line  $T_c(x)$ . Recently this consistency, together with a finite-size effect observed in the temperature dependence of  $\lambda$  close to  $T_c$ , was used to derive the amplitude of the perpendicular real-space phase correlation length  $\xi_{c0}^{\phi}$  as a function of doping for the same series of samples.<sup>48</sup>

### C. $n_s/m^*$

On a microscopic basis,  $\lambda$  is related to other parameters of the superconducting state, such as the superfluid density  $n_s$  (not to be confused with the carrier density) and the effective mass of the carriers  $m^*$ :  $\lambda^{-2} \propto n_s/m^*$ . This raises the ques-

tion whether the superfluid density  $n_s$  or the effective mass  $m^*$  is responsible for the increase of  $\lambda$  as doping proceeds beyond the optimum value. Various possibilities have already been suggested.<sup>1,40</sup> To go beyond these arguments, the question to be addressed is whether these additional carriers introduced in the system beyond optimum doping all contribute to the superfluid, i.e., whether  $n_s \rightarrow n$  at zero temperature and/or whether microscopic phenomena (on length scales smaller than  $\lambda$ ), such as a *chemical* or an *electronic phase separation*,<sup>49</sup> could actually lower  $n_s$ . An analysis of the optical conductivity,<sup>50</sup> the <sup>63</sup>Cu relaxation rate, the <sup>63</sup>Cu Knight shift,<sup>51</sup> and of the specific heat<sup>52</sup> suggests that the added carriers in the overdoped regime only partially condense into pairs.

## VII. CONCLUSIONS

We have shown that the epitaxial driving force imposes a residual tension on the 214 thin films grown on SrTiO<sub>3</sub>. This tension has significant effects on both the normal state and the superconducting properties of these films, mainly by increasing the resistivity and decreasing the critical temperature. Measurements of the penetration depth as a function of doping reveal a nonmonotonic dependence, previously not observed in this compound. After completion of this work, we have been informed that  $\mu\text{SR}$  measurements of the doping dependence of  $\lambda$  in bulk 214 compounds<sup>53</sup> are fully consistent with our observations.

## ACKNOWLEDGMENTS

The authors wish to thank K. A. Müller, J. G. Bednorz, J.-M. Triscone, D. Ariosa, R. Micnas, J. J. Rodríguez-Núñez, and C. Rossel for stimulating discussions, and the Swiss National Science Foundation for financial support through the PNR30 program. M. Pedersen, K. Kitazawa, and S. Ushida have contributed considerably towards the understanding of the behavior of overdoped compounds. We also thank I. Mangelschots and K. Ishida for relating the NMR data to our results.

\*Corresponding author, electronic address: loc@zurich.ibm.com

<sup>1</sup>Y. J. Uemura *et al.*, Nature (London) **364**, 605 (1993).

<sup>2</sup>C. Niedermeier *et al.* (unpublished); C. Niedermeier *et al.*, Phys. Rev. Lett. **71**, 1764 (1993).

<sup>3</sup>Y. J. Uemura *et al.*, Phys. Rev. Lett. **62**, 2317 (1989); Phys. Rev. B **38**, 909 (1988).

<sup>4</sup>T. Schibauchi *et al.*, Phys. Rev. Lett. **72**, 2263 (1994).

<sup>5</sup>T. Schneider *et al.*, Physica C **216**, 432 (1993); T. Schneider, Proc. SPIE **2157**, 2 (1994).

<sup>6</sup>C. Bernhard *et al.*, Phys. Rev. B **52**, 10 488 (1995).

<sup>7</sup>J. G. Bednorz and K. A. Müller, Z. Phys. B **64**, 189 (1986).

<sup>8</sup>K. Kitazawa *et al.*, Appl. Supercond. **1**, 567 (1993); T. Nagano *et al.*, Phys. Rev. B **48**, 9689 (1993).

<sup>9</sup>P. G. Radaelli *et al.*, Phys. Rev. B **49**, 4163 (1994).

<sup>10</sup>R. B. Van Dover *et al.*, Phys. Rev. B **35**, 5337 (1987); K. Yoshimura *et al.*, J. Phys. Soc. Jpn. **59**, 3073 (1990).

<sup>11</sup>D. R. Harshman and A. P. Mills, Jr., Phys. Rev. B **45**, 10 684 (1992).

<sup>12</sup>Y. Jaccard *et al.*, Proc. SPIE **2158**, 200 (1994); Physica C **235–240**, 1811 (1994).

<sup>13</sup>E. J. Williams *et al.*, in *Electron Microscopy & Analysis 1993*, edited by A. Craven, IOP Conf. Proc. No. 138 (Institute of Physics and Physical Society, London, 1994), p. 329; E. J. Williams *et al.*, *Proceedings of the 13th Int'l Congress on Electron Microscopy (ICEM13), Paris, France, July 1994*, edited by B. Jouffrey, C. Colliex, J. P. Chevalier, F. Glas, and P. W. Hawkes (Les Editions de Physique, Paris, 1994), Vol. 2A, p. 987.

<sup>14</sup>M. Suzuki, Phys. Rev. B **39**, 2312 (1989); M. Suzuki and M. Hikita, *ibid.* **44**, 249 (1991).

<sup>15</sup>H. Y. Hwang, B. Batlogg, H. Takagi, H. L. Kao, J. Kwo, R. J. Cava, J. J. Krajewski, and W. F. Peck, Jr., Phys. Rev. Lett. **72**, 2636 (1994).

<sup>16</sup>H. Takagi *et al.*, Phys. Rev. Lett. **69**, 2975 (1992).

<sup>17</sup>H. L. Kao *et al.*, Appl. Phys. Lett. **59**, 2748 (1991).

<sup>18</sup>Y.-Q. Song *et al.*, Phys. Rev. Lett. **70**, 3131 (1993).

<sup>19</sup>M. Takigawa *et al.*, Phys. Rev. B **43**, 247 (1991).

<sup>20</sup>K. Fujiwara *et al.*, Physica C **184**, 207 (1991); K. Fujiwara *et al.*, J. Phys. Soc. Jpn. **59**, 3459 (1990).

<sup>21</sup>Y. Itoh *et al.*, J. Phys. Soc. Jpn. **63**, 22 (1994).

- <sup>22</sup>H. Takagi *et al.*, Phys. Rev. B **40**, 2254 (1989).
- <sup>23</sup>G. Rietveld, M. Glastra, and D. van der Marel, Physica C **241**, 257 (1995).
- <sup>24</sup>J. S. Schilling and S. Klotz, in *Physical Properties of High Temperature Superconductors*, Vol. 3, edited by D. M. Ginsberg (World Scientific, London, 1992), p. 59.
- <sup>25</sup>J.-P. Locquet *et al.* (unpublished).
- <sup>26</sup>H. J. Scheel, Mater Res. Bull. **19**, 26 (1994).
- <sup>27</sup>F. Tresse, Ph.D. thesis, University of Bordeaux, France, 1990.
- <sup>28</sup>E. J. Williams *et al.*, *Proceedings of Microscopy and Microanalysis*, edited by G. W. Bailey *et al.* (Jones & Begell, New York, 1995), p. 382.
- <sup>29</sup>H. Takahashi *et al.*, Phys. Rev. B **50**, 3227 (1994).
- <sup>30</sup>J. B. Goodenough and A. Manthiram, J. Solid State Chem. **88**, 115 (1990).
- <sup>31</sup>N. Tanahashi *et al.*, Jpn. J. Appl. Phys. Lett. **28**, L762 (1989).
- <sup>32</sup>F. Arrouy *et al.*, this issue, Phys. Rev. B **54**, 7512 (1996).
- <sup>33</sup>Wu. Ting and K. Fossheim, Phys. Rev. B **48**, 16 751 (1993).
- <sup>34</sup>Y. Motoi *et al.*, J. Phys. Soc. Jpn. **60**, 384 (1991).
- <sup>35</sup>Y. Maeno *et al.*, in *Advances in Superconductivity VI*, edited by T. Fujita and Y. Shiohara (Springer-Verlag, Tokyo, 1994), p. 103.
- <sup>36</sup>C. Meingast *et al.*, Physica C **235-240**, 1313 (1994); F. Gugenberger *et al.*, Phys. Rev. B **49**, 13 137 (1994).
- <sup>37</sup>M. Braden *et al.*, Phys. Rev. B **47**, 12 288 (1993).
- <sup>38</sup>S. L. Bud'ko *et al.*, Phys. Rev. B **46**, 1257 (1992).
- <sup>39</sup>M. Z. Cieplack *et al.*, Appl. Phys. Lett. **65**, 3383 (1994).
- <sup>40</sup>Q. Li *et al.*, Phys. Rev. B **47**, 2854 (1993).
- <sup>41</sup>S. M. Anlage *et al.*, Appl. Phys. Lett. **54**, 2710 (1989).
- <sup>42</sup>B. Jeanneret *et al.*, Appl. Phys. Lett. **55**, 2336 (1989).
- <sup>43</sup>M. V. Feigel'man, V. B. Geshkenbein, and A. I. Larkin, Physica C **167**, 177 (1990).
- <sup>44</sup>O. Brunner *et al.*, Phys. Rev. Lett. **67**, 1354 (1991).
- <sup>45</sup>G. Blatter, M. V. Feigel'man, V. B. Geshkenbein, A. I. Larkin, and V. M. Vinokur (unpublished).
- <sup>46</sup>M. Gurvitch and A. T. Fiory, Phys. Rev. Lett. **59**, 1337 (1987).
- <sup>47</sup>F. Gao *et al.*, Phys. Rev. B **47**, 1036 (1993).
- <sup>48</sup>Y. Jaccard *et al.*, Europhys. Lett. **34**, 281 (1996).
- <sup>49</sup>K. A. Müller, in *Phase Separation in Cuprate Superconductors*, edited by K. A. Müller and G. Benedek, The Science and Culture Series: Physics, Proceedings of the Int'l School of Solid State Physics – 3rd Workshop, Erice, Italy (World Scientific, Singapore, 1993), and references therein.
- <sup>50</sup>S. Uchida, *et al.*, J. Low Temp. Phys. **95**, 109 (1994).
- <sup>51</sup>S. Ohsugi, *et al.*, J. Phys. Soc. Jpn. **63**, 700 (1994).
- <sup>52</sup>J. W. Loram, *et al.*, Physica C **235-240**, 134 (1994).
- <sup>53</sup>H. Keller, *et al.* (private communication).